1-1-2018

Superelastic Hybrid CNT/Graphene Fibers for Wearable Energy Storage

Zan Lu
University of Wollongong

Javad Foroughi
University of Wollongong, foroughi@uow.edu.au

Caiyun Wang
University of Wollongong, caiyun@uow.edu.au

Hairu Long
Donghua University

Gordon G. Wallace
University of Wollongong, gwallace@uow.edu.au

Superelastic Hybrid CNT/Graphene Fibers for Wearable Energy Storage

Abstract

The demands for wearable technologies continue to grow and novel approaches for powering these devices are being enabled by the advent of new electromaterials and novel fabrication strategies. Herein, a novel approach is reported to develop superelastic wet-spun hybrid carbon nanotube graphene fibers followed by electrodeposition of polyaniline to achieve a high-performance fiber-based supercapacitor. It is found that the specific capacitance of hybrid carbon nanotube (CNT)/graphene fiber is enhanced up to ≈39% using a graphene to CNT fiber ratio of 1:3. Fabrication of spring-like coiled fiber coated with an elastic polymer shows an extraordinary elasticity capable of 800% strain while affording a specific capacitance of ≈138 F g -1 . The elastic rubber coating enables extreme stretchability and enabling cycles with up to 500% strain for thousands of cycles with no significant change in its performance. Multiple supercapacitors can be easily assembled in series or parallel to meet specific energy and power needs.

Disciplines

Engineering | Physical Sciences and Mathematics

Publication Details

Lu, Z., Foroughi, J., Wang, C., Long, H. & Wallace, G. G. (2018). Superelastic Hybrid CNT/Graphene Fibers for Wearable Energy Storage. Advanced Energy Materials, 8 (8), 1702047-1-1702047-10.

Article type: Full Paper

Superelastic Hybrid CNT/Graphene Fibers for Wearable Energy Storage

Zan Lu, Javad Foroughi*, Caiyun Wang, Hairu Long, Gordon G. Wallace*

Z. Lu, Prof. H. Long
College of Textiles
Engineering Research Center of Technical Textile
Donghua University
Shanghai 201620, China

Z. Lu, Dr. J. Foroughi, Dr. C. Wang, Prof. G. G. Wallace
Intelligent Polymer Research Institute
ARC Centre of Excellence for Electromaterials Science
University of Wollongong
Wollongong, NSW 2522, Australia
Email: foroughi@uow.edu.au, gwallace@uow.edu.au

Dr. J. Foroughi
Illawarra Health and Medical Research Institute
University of Wollongong
Wollongong, NSW 2522, Australia

Abstract

The demands for wearable technologies will continue to grow and novel approaches for powering these devices are being enabled by the advent of new electromaterials and novel fabrication strategies. Herein, a novel approach is reported to develop superelastic wet-spun hybrid carbon nanotube graphene fibers followed by electrodeposition of polyaniline to achieve a high-performance fiber-based supercapacitor. It is found that the specific capacitance of hybrid carbon nanotube (CNT)/graphene fiber is enhanced up to ~39% using a graphene to CNT fiber ratio of 1:3. Fabrication of spring-like coiled fiber coated with an elastic polymer shows an extraordinary elasticity capable of 800% strain while affording a specific capacitance of ~138 F g^{-1}. The elastic rubber coating enabled extreme stretchability and enabling cycles with up to 500% strain for thousands of cycles with no significant change in its performance.

Multiple supercapacitors can be easily assembled in series or parallel to meet specific energy and power needs.

1. Introduction

The study of wearable energy storage devices has been undertaken by researchers around the world in recent decades in a quest to meet growing demands in the field of biomedical devices as well as communication and entertainment systems.[1, 2] Stretchable and bendable supercapacitors or batteries are two typical energy storage devices used in practical applications.[3, 4] The composition and structure of materials used are critical in determining stretchability.[5] Developing intrinsically elastic active materials should enable the realisation of stretchable supercapacitors or batteries. However, existing active materials utilized in energy storage suffer from poor elasticity or relatively low electrochemical performance. In previous studies three major stretchable structures have been proposed: coiled fiber structure,[6-8] wavy structure[5, 9, 10] and island-bridge structure.[11-13] The active materials applied in these structures should be easily handled and tough. For use in wavy and island-bridge structures soft materials are required. Coating, transferring, in-situ deposition or polymerization of active materials onto a stretchable substrate such as fabric, polymer and paper have been devised for the electrodes of energy storage and conversion devices; but mostly declaring a low elasticity.[14, 15]

A fiber-based or wire-shaped device can be easily integrated into stretchable yarns or fabrics to fulfil a more practical demand of wearable energy storage, conversation or transition in our daily life. The electrochemical property and stretchability both play a vital role in the fiber-based supercapacitors and batteries.[16-18] Carbon nanotubes (CNT) are widely used electrode materials that possess extraordinary physical and chemical properties, and they have also been verified to assemble into fiber formation by using solid-state spun or wet-spun techniques.[19] Fibers formed by pristine CNT have been demonstrated with high electrical conductivity and

superior mechanical properties, although the intrinsic electrochemical performances of CNT fibers are not outstanding enough.[20-23] A possible explanation of this behaviour lies in the strong interaction between carbon nanotubes, which, while increasing the packing density inside fibers, does not allow high ion accessibility. To reduce the dense stacking, CNT/Graphene composites have been proposed and fabricated to increase inner porosity.[24, 25] On the other hand, coiled structure and elastic polymer fibers have been reported previously as the most popular approach or material to enhance the stretchability of fibers and films, which have been incorporated with various active materials such as carbon nanomaterials (e.g., nanotubes, graphene), metal oxide nanoparticles and conductive polymers.[6, 15, 26-28] The reported coiled fiber supercapacitor only afforded up to a strain of 150% to maintain its performance,[6] although the capacitance could be achieved as high as 382 mF cm^{-2}.[28] Coincidentally, the psudocapacitance material, deposited carbon nanotube sheets wrapped coaxial elastic fiber, demonstrated a high specific capacitance as well as a strain of 400% without damages to the properties.[27]

In this paper, we explore a novel approach to fabricate nanostructured carbon nanotube/graphene/ conducting polymer nanocomposite fiber as superelastic fiber-based supercapacitor. As-prepared wet-spun CNT/Graphene fibers have been used to develop hybrid CNT/Graphene/conducting polymer (PANi) using electrodeposition. A mandrel coiled CNT/Graphene/PANi fiber (springlike) was fabricated and coated with PVA/H_3PO_4 followed by covering with highly stretchable polymer to achieve a relatively high electrochemical performance combined with an excellent elasticity of 800% strain. The wire-shaped supercapacitor affords a practical potential candidate in the energy storage applications of wearable wrist band, smart watch and finger sensor etc. The hybrid fibers exhibited improved stretchability and electrochemical properties as compared with the pristine CNT material, conducting polymer and graphene fibers. The nanocomposite fibers can be used for

applications where the electrical conductivity, along with stretchability and excellent electrochemical properties, are of primary importance.

2. Results and discussions

To develop the superelastic fiber-based supercapacitor, wet-spun pristine CNT and hybrid CNT/Graphene fibers have been produced via wet-spinning. The thermal exfoliation of graphene and liquid-crystal of single-walled carbon nanotube were used to prepare the spinning solution. The fabrication process for the wet-spun hybrid CNT/Graphene fiber is schematically illustrated in **Figure 1**. To reduce the layer number in the exfoliated graphene, multi-layer graphene platelets were used as raw materials and subjected to further exfoliation. Figure 1a and b present the photographs of graphene platelets before and after treatment, respectively. As a result of treatment with CSA and H_2O_2, an immediate dramatic volume expansion of multi-layers of the graphene could be achieved.[29, 30] After washing and freeze drying, the sponge-like graphene sheets (Figure 1c) were redispersed in CSA with the assistance of ultrasonication.[31]

The graphene flakes obtained can form an extraordinary highly concentrated dispersion (20 mg mL^{-1}) in CSA without any visible aggregation and can be mixed with single-walled carbon nanotubes as a spinnable liquid-crystal solution, as we previously reported.[19] The continuous and scalable fiber can be collected by extruding the spinning dope into a coagulation bath with following wash procedure (Figure 1e-f). The diameter of prepared CNT/Graphene nanocomposite fiber, which ranged from around 60 μm to 120 μm, can be controlled by using different gauge of syringe needles from 25G to 22G. The fiber was extremely flexible and could be easily tied with a knot and twisted as a two-ply yarn, shown in **Figure S1**.

SEM micrographs of the pristine CNT and CNT/Graphene fibers are shown in **Figure 2** (a-f). As can be seen from the cross-section morphology (Figure 2a-b), the wet-spun pristine CNT

fiber presents a smooth cross-section with neat CNT bundles along the fiber. The cross-section of the as-prepared CNT/graphene fiber (Figure 2c-d) was examined and the morphology was found to be completely different from the pristine CNT fiber. The graphene sheets are clearly seen in the cross-section of CNT/Graphene fiber in Figure 2d and form a layer-by-layer structure with the continuous single-walled carbon nanotubes bundles. The SEM images of the cross-section of CNT/Graphene fiber in wet-state shows that the as-prepared CNT/Graphene fiber has a porous structure (Figure 2e, f), this morphology shrunk to form the wrinkled CNT layer-by-layer structure after drying in an oven.

To evaluate the effect of the graphene ratio on electrochemical performance of the hybrid CNT/Graphene fiber, the hybrid CNT fiber was prepared with five different ratios of graphene (from 0 to 50%). The cyclic voltammetry (CV) curves for pristine CNT fiber and hybrid CNT/Graphene fibers with different ratios of graphene were compared at a 50 mV S^{-1} scan rate using a three-electrode system (Figure 2g). With increasing percentage of graphene sheets in the CNT/Graphene hybrid fiber, the areas of the CV curves are similar from the proportion of 0 to 25% and then significantly enlarged at the percentage of 33.3% with subsequent decrease at 50%.

As can be seen from Figure 2g, the as-prepared pristine CNT fiber shows a voltammetric response due to redox reactions underwent by oxygen containing functional groups which were mainly generated during the nanotubes' purification step in nitric acid by the manufacturer.[21, 32, 33] It is notable that the redox peaks become inconspicuous with the decrease in ratio of the CNT in the hybrid fiber, indicating that the CSA treatment would not introduce oxygen groups on graphene during the spinning procedure. Furthermore, the electrical conductivity of as-prepared hybrid fibers had been evaluated as a function of graphene ratio in the fiber under laboratory humidity and temperature conditions by an in-house linear four-point probe cell. As can be seen from Figure 2h, the electrical conductivity of the hybrid CNT/Graphene fiber

decreased as a result of increasing graphene ratio. A high-resolution SEM cross-section image of the pristine CNT fiber (Figure 2 b) shows closely packed CNT bundles, which implies an effective electron pathway for longitudinal current collection. However, the hybrid CNT/Graphene fiber (Figure 2 d) shows a porous structure which could affect the electron pathway and suffer lower electrical conductivity compared with the pristine CNT fiber. To explain this phenomenon, as previously reported the monolayer graphene sheets have a large electroactive surface area and excellent electrical properties than multi-layer graphene. The stacked graphene sheets inside the hybrid fiber accordingly block the existing electronic channels of CNT fiber and result in the worse electrical conductivity with graphene increasing. Therefore, to transfer the excellent mechanical and physical properties of individual graphene to macrostructures for practical application remains a challenge.[34, 35]

On the other hand, the capacitances of the as-prepared fibers were obtained from the CV curves (Figure 2g) which show that the highest capacitance that can be achieved was ~50 F g^{-1}. This value is about ~39% higher than the pristine CNT fiber (Supporting information, **Figure S2**). Adding graphene sheets up to ~33 % into the hybrid fiber could contribute towards producing a hybrid fiber with a porous structure that could enhance fast ion diffusion during electrochemical performance. Interestingly, the amount of graphene flakes added below 33% cannot separate the CNT bundles to form a porous structure (Supporting information, Figure S2a, b), and above this value the pores inside the fiber will be blocked by graphene as shown in Figure S2c, d.

The hybrid CNT/Graphene fiber based supercapacitors had limited capacitances because their active material was based on CNT and graphene; totally depending on the electrochemical double-layer capacitance energy storage mechanism. To enhance the capacitance of our fiber-based supercapacitor to make it more practical in applications, pseudocapacitive materials deposited CNT/Graphene composite fibers, as promising electrodes and skeleton for

structuring stretchable and highly performing supercapacitors, were developed. The combination of carbon nanotubes, graphene and conducting polymer fibers led to the development of high performance electrodes for supercapacitors and batteries.[36] Pseudocapacitors based on conducting polymers offer low cost, high specific energy and power, high conductivity, lightweight and enhanced flexibility over other pseudocapacitive materials.[37] Consequently, polyaniline (PANi) as an outstanding electrochemical material has been used to develop pseudocapacitive CNT/Graphene hybrid fibre based supercapacitors. Hybrid pseudocapacitive fiber based supercapacitor was obtained by electrochemical polymerization of aniline on the surface and within the porous hybrid CNT/Graphene fibre. The as-prepared CNT/Graphene hybrid fiber with the graphene ratio of ~33%, being the optimized hybrid fiber with the highest electrochemical performance, was chosen to obtain high capacitive CNT/Graphene/PANi hybrid fiber. Because only nanostructured surfaces of PANi can participate in the electrochemical energy storage reaction, the loading amount of PANi was controlled by adjusting its deposition time to have a thin shell with reasonable thickness (~200 nm) to obtain high capacitances and high-rate capability, simultaneously. Consequently, the impact of the PANi electrodeposition time on the electrochemical properties of a single fiber has been investigated. The weight of deposited PANi was calculated before and after electrodeposition using a high-precision balance (**Figure S4** the Supporting Information). SEM images of our novel CNT/graphene/PANi hybrid fiber are shown in **Figure 3**. The aligned CNT bundles can be observed clearly on the surface of the fiber without deposition in Figure 3a. After PANi deposition (Figure 3b, c and d), a mesoporous film, which is morphologically characteristic of conducting polymer,[38] was uniformly formed on the surface of the hybrid fiber. A high-resolution SEM cross-section image of the core (CNT/Graphene)-shell (PANi) hybrid fiber is shown in Figure 3e, f with a shell thickness of over a hundred nanometres (~200 nm). In addition, the redox peaks of PANi are becoming

more significant (in Figure 3g) with increasing electrodeposition time, which is due to the larger amount of PANi involved in the redox reactions. Accordingly, the enclosed cyclic voltammogram areas increased as the PANi deposition time rose to 5 min and then decreased with continuous electrodeposition. Meanwhile, specific capacitances of the composites fibers dropped noticeably after depositing 8 min of PANi (in Figure 3h). This trend could be ascribed to the excess PANi coated on the outer surface of the hybrid fiber, which could not effectively contact with the fiber, leading to a slower and less effective ion diffusion.[39] The highest specific capacitance of ~226 F g^{-1} at a scan rate of 10 mV s^{-1} was achieved for the developed fiber based supercapacitor with 5 min electrodeposition of PANi. Despite the low amount of PANi, it dominated the charge storage capacity; the area of the CV obtained after PANi deposition was about 565 % larger than for the hybrid CNT/graphene fiber alone. The high electrochemically active surface area provided by the hybrid CNT/graphene nanostructure together with the effective pseudocapacitive decoration of PANi have enabled such high capacitances to be obtained. It should be noted that the specific capacitances of CNT/Graphene/PANi hybrid fibers decreased at fast scan rates, especially for the fibers with more PANi deposition time (5 and 8 min).

To develop superelastic fiber-based supercapacitor (FSC), the as-prepared hybrid CNT/Graphene fiber with PANi (deposition time was 5 min) was selected as a platform to create the device. Highly stretchable styrene-(ethylene-butylene)-styrene (SEBS) based polymer was used to provide the whole device with an outstanding elongation property. The SEBS rubber itself could be stretched as high as 900% elongation (Supporting information, **Figure S5**). The fabrication of the stretchable device is schematically shown in **Figure 4**. Two symmetrical CNT/graphene/PANi hybrid fibres based supercapacitor were coated with an aqueous PVA-H_3PO_4 gel electrolyte and twisted together to complete the assembly of the solid-state supercapacitors. Then the as-prepared fiber-based supercapacitor was firstly mandrel

coiled on a stainless steel rod, followed by casting a thin layer of rubber which was dissolved in cyclohexane to fix a springlike structure of the supercapacitor. The device was then removed from the steel rod and mounted in a cylindrical mould to be thoroughly covered with the rubber solution. The coated polymer could be solidified in air quickly and afforded a good protection to the device without significantly influencing detrimentally the electrochemical properties of the device. Theoretically, the spring-structure supercapacitor can be extended to its original length and the tensile elongation also can be controlled by the diameter and density of the coiled.[40] As can be seen from Figure 4b the fabricated ultra-stretchable solid-state supercapacitor had a capability to elongate up to 800%

CV curves (**Figure 5a**) for the CNT/Graphene/PANi hybrid fiber-based supercapacitor were measured using scan rates from 10 to 200 mV s^{-1}, to provide the specific capacitances. The cyclic voltammograms could maintain a rectangular shape at a scan rate of 100 mV s^{-1} but showed an unsatisfactory deformation when the scan rate was over 200 mV s^{-1}, indicating a poor rate property of polyaniline deposited hybrid fiber-based supercapacitor compared with that of pristine CNT fiber supercapacitor in our previous work. This phenomenon is firstly ascribed to the formation of graphene sheet inside the fiber. On the one hand, the large stacked sheets of impermeable graphene can significantly reduce the effective diffusion coefficient. On the other hand, the graphene inside tend to be parallel to each other to form a sheet-like channel that hinders the diffusion of the ions in the solid-state electrolyte. Secondly, the ion channels throughout the porous fiber blocked by thick PANi layer also leading to a slow diffusion of ions.[41] Effect of static mechanical deformations on the electrochemical performance of the fabricated hybrid fiber based supercapacitors were evaluated under various strains. The application of static tensile strains of 0%, 100%, 200%, 300%, 400%, 500%, 600%, 700% and 800% resulted in negligible changes in the CV curves measured at a scan rate of 20 mV s^{-1} (Figure 5b). As expected, the springlike structure, as well as the introduction of SEBS rubber,

had no obvious effects on the electrochemical properties of the developed device. Consequently, the fabricated fiber based supercapacitors afforded retention of specific capacitance of 99.2% at 800% strain. This value is 413% higher than the capacitance retention of the CNT/MnO_2/rubber coiled fiber which had been reported recently.[42]

The galvanostatic charge–discharge processes (Figure 5c) were carried out at an increasing current density from 0.2, 0.5, 1, 2, 3, 5 to 8 A g^{-1}. Triangle-shaped galvanostatic charge-discharge curves for various current densities were consistent with the quasi-capacitive performance of the hybrid fiber based supercapacitor. The ultra-stretchable hybrid fiber supercapacitors were able to achieve a specific capacitance of 182.6 F g^{-1} at the current density of 0.2 A g^{-1} and maintained 23.8 F g^{-1} at 8 A g^{-1}. The almost symmetric curves were well maintained and exhibited indistinctive IR drop, and afforded good Coulombic efficiencies of 95% and 98% at 0.2 A g^{-1} and 8 A g^{-1}, respectively.[39, 43] Figure 5d shows galvanostatic charge–discharge profiles with increasing strains to 800%, and the specific capacitances remained almost unchanged. To investigate the stability of the superelastic fiber-based supercapacitor, a cyclic charge–discharge characterization was carried out at a current density of 1 A g^{-1} (Figure 5e), and the specific capacitances retention was 77.3% after 5,000 cycles with 800% strain. The results in Figure 5f show the dependence of specific capacitance on stretch cycle number with increasing tensile strains from 100% to 500%, and the capacitance was retained after 5,000 stretching cycles.

Electrochemical impedance spectroscopy (EIS) was carried out to study the electrochemical performance of the stretchable fiber-based supercapacitor with various elongated lengths. The ohmic resistance of the selected supercapacitor obtained from the x-intercept of the Nyquist plot in **Figure S6** was around 300 Ω, which was higher than that of a pure CNT fiber based supercapacitor in our previous work. At high frequencies, the resistance can be manifested as a semi-circle or arc; however, these shapes were not significant in the curves which indicates

that the contact resistance between deposited PANi and CNT/Graphene fiber surface are minimal. With the increasing elongation of supercapacitor, the linear slopes of the curves are changing slightly at low frequencies, indicating a good stability of electrochemical property under different strains.

These trends are also supported by the Bode plots calculated from EIS data shown in Figure 2. The real and imaginary parts of the gravimetric capacitance can be calculated from the Nyquist plots by using the equations

$$C_g' = \frac{-Z''(\omega)}{m\omega|Z(\omega)|^2}$$

$$C_g'' = \frac{-Z'(\omega)}{m\omega|Z(\omega)|^2}$$

where Cg′ and Cg″ are the real and imaginary parts of gravimetric specific capacitance; Z′ and Z″ are the real and imaginary parts of impedance (Z); m is the mass of the fiber electrode; and ω = 2πf is the radial frequency. It is evident that the gravimetric specific capacitances at different frequencies for the stretchable supercapacitor almost have no change compared with the original length device in **Figure S7a**. For the supercapacitor at the applied strain from 100% to 800% shown in Figure S7b, the location of feature peak shows the same from that of un-stretched supercapacitor with time constant of 6.76 s at 0.148 Hz. All the variations in an increasing trend with the elongations of the supercapacitor is in a good agreement with CV and galvanostatic charge-discharge cycling results.

Although the above results show that tensile strains have little effect on capacitance, it is also important to evaluate how prolonged tensile strain affects the stability of the device when undergoing dynamic electrochemical performance testing. The application of prolonged (up to 96 hours) tensile strain of 400% resulted in negligible changes in the CV curves measured at a scan rate of 20 mV s^{-1} in a two-electrode system (**Figure S8**). The fabricated supercapacitor device provided about 78% capacitance retention at 400% tensile strain while the device

showed a 75% elongation after 4 days' long-time tensile strain (in **Figure S9**). Although the rubber itself exhibits a creep, the device reverts to a 20% length increase of the original length after one day of free standing, due to the permanent deformation of the spring structure. Stress relaxation characteristics were measured (illustrated in **Figure S10**) and revealed a larger drop of stress can be observed under higher strain, while 100% tensile strain showed a stable stress after holding for 10 min. In addition, it was found that the 400% and 800% tensile strain exhibited a linear trend of decrease after about 50 min and 100 min respectively, demonstrating excellent relaxation resistance. In other words, the stretched supercapacitor can steadily maintain a force inside to retain shape over a long period of strain. Furthermore, stress-strain curves were observed on unloading and reloading a fabricated supercapacitor device over an 800% strain range. As can be seen from **Figure S11**, a linear trend with elastic deformation from 0 to 500% tensile strain was observed while some hysteresis can be observed for the tensile strains over 500%. Consequently, the supercapacitor coated with SEBS rubber provides excellent mechanical properties of a viscoelasticity material[44] which could be developed into an ultra-stretchable structure for the fabricated hybrid CNT/Graphene/PANi fiber supercapacitor.

The specific capacitance and stretchability of this device and previous stretchable supercapacitors are compared in **Table 1**, and the data is illustrated in **Figure 6**. The fiber based supercapacitor exhibits a relatively high specific capacitance based on the mass of a single electrode with elongation capabilities almost twice that of previous reports.[27] Multiple supercapacitors can be easily assembled in series or parallel to meet specific energy and power needs for practical applications (**Figure 7a, c**). As shown in Figure 7b and d, the potential output of the cyclic voltammogram is tripled when three individual devices are connected in series, while the detected current increased by an order of three when three devices are connected in parallel. In addition, a sealed stretchable supercapacitor with four devices in series

can be further applied in wearable energy storage, such as a ring or a wrist band (Figure 7e, f, g). Moreover, the wire-shaped multi-assembled supercapacitor also has a potential to be integrated in a stretchable textile (Figure 7 h, i). The textile can be integrated with soft and stretchable silicone material to provide protection from the environment including washing (Figure 7j, k and l).

3. Conclusion

In summary, a nanostructured CNT/graphene hybrid fiber has been developed with a view to enhance both the electrochemical and mechanical properties of the wet-spun fiber through a wet-spinning process. It was found that the specific capacitance of the wet-spun CNT/graphene fiber could be improved by 39% when the ratio of graphene wet-spun CNT fibers reached ~33% w/w. The conducting polymer PANi acting as a pseudocapacitive material, was electrochemically deposited onto the wet-spun CNT/graphene fiber. An ultra-stretchable fiber based supercapacitor has been developed, which exhibited an extraordinary high elasticity of over 800% tensile strain with a high specific capacitance of 138 F g^{-1} at a discharge current density of 1 A g^{-1}. Excellent capacitance retention of ~106 F g^{-1} after 5,000 cycles over 800% elongation cycles was observed. The capacitance decreased to 78% of the original after four day's prolonged strain at 400% elongation. The developed superelastic fiber-based supercapacitor can be easily fabricated into various shapes and widely used in practical structures including wearable devices.

4. Experimental Section

Fabrication of graphene: The Graphene sheets were prepared as previously reported[29]. Multi-layer Graphene platelets (Cheaptube Co., Ltd, 10-12 layers), Chlorosulfonic acid (CSA, Sigma Aldrich, 99.9 wt%) and H_2O_2 (30%, Chem-supply) were used as received without further purification. 100 mg of graphene platelets were added to 10 mL of CSA solution and stirred overnight to ensure that CSA was totally intercalated in the space of each layer. Then,

6 mL of H_2O_2 was added to the solution dropwise under stirring. The graphene was harvested by centrifugation, followed by washing several times with distilled water to remove the excess acids. After that, the products were freeze-dried under vacuum.

Preparation of pristine CNT fiber and hybrid CNT/Graphene fibers: SWNTs were used as purchased (Nano-lab, USA), different ratios of SWNTs and graphene were mixed in 1 ml chlorosulfonic acid by using Thinky ARE-250 mixer for 20 min. The amounts of graphene contained in the spinning solution was 0%, 11.1%, 16.7%, 25%, 33.3% and 50%. The spinning dope was transferred into a 5 ml glass syringe with 22G needle then pump extruded into an acetone bath at a fixed rate of 25 ml/h and the rotating speed was 20 rpm. The prepared wet-spun CNT and hybrid CNT/graphene fibers were then washed with distilled water for three times and dried in an oven at 120 ℃.

Preparation of PANi deposited CNT/Graphene hybrid fibers and electrochemical performance measurement: The PANI was electrochemically deposited on CNT/Graphene fibers in an electrolyte of 1M H_2SO_4 and 0.1 M Aniline monomer (Sigma Aldrich) at a potential of 0.75V with a three-electrode system (eDAQ, Australia), using Ag/AgCl as the reference electrode and Pt mesh as the counter electrode. After electrodeposition, the as-prepared fibers were washed with ethanol and distilled water several times and dried at 70 ℃ in an oven. The cyclic voltammetry (CV) of the fibers was performed in 1M H_2SO_4 (CHI 660E, USA) at room temperature, and galvanostatic charge/discharge tests were measured using a battery test system (Neware Electronic Co.) from 0 to 0.8V. Electrochemical impedance spectra (EIS, Gamry EIS 3000 system) were obtained in the frequency range of 100 kHz to 0.01 Hz with an AC perturbation of 10 mV at open circuit potential.

Fabrication of highly stretchable solid-state supercapacitor: PVA-H_3PO_4 gel electrolyte was prepared by mixing 3g PVA (Sigma Aldrich, Mwt 124-186k) with 3g H_3PO_4 (Sigma Aldrich) in 30 mL Milli-Q water and stirring at 90℃ until the solution became transparent.

Two prepared CNT/Graphene/PANi hybrid fibers were coated with this solid electrolyte several times and dried for 1 h each time. Then, two PVA-H_3PO_4 coated fibers were twisted slightly and each end of the electrode was extended with a stainless-steel wire and finally coated with PVA-H_3PO_4 along the twisted part to obtain a solid-state fiber-based supercapacitor (FSC).

Fabrication of superelastic fiber-based supercapacitor: as-prepared electrolyte (PVA-H_3PO_4) coated hybrid CNT/graphene/PANi fiber was used to fabricate a mandrel coiled fiber. A springlike structure of the fiber was fixed in a mould and thoroughly coated with rubber solution, then left in air until the rubber solidified. The rubber solution was prepared by mixing commercial SEBS rubber 50% (w/w) with cyclohexane (Sigma Aldrich, 99%).

Supporting Information

Supporting Information is available from the Wiley Online Library or from the author.

Acknowledgements

This work has been supported by the Australian Research Council under the Discovery Early Career Researcher Award (J. Foroughi, DE12010517), the Australian Research Council Centre of Excellence Scheme (Project Number CE 140100012) and the Australian Laureate Fellowship scheme (FL110100196). Zan Lu acknowledges the support of CSC scholarships from the Ministry of Education of P. R. China. The authors acknowledge AIIM (Australian Institute for Innovative Materials) funding (AIIM for Gold), the use of facilities within the UOW Electron Microscopy Centre, and the Australian National Nanofabrication Facility-Materials Node (ANFF).

References

[1] J. A. Rogers, T. Someya, Y. Huang, *Science* **2010**, 327, 1603.
[2] D. J. Lipomi, Z. Bao, *Energ. Environ. SCI.* **2011**, 4, 3314.
[3] N. S. Choi, Z. Chen, S. A. Freunberger, X. Ji, Y. K. Sun, K. Amine, G. Yushin, L. F. Nazar, J. Cho, P. G. Bruce, *Angew. Chem. Int. Ed.* **2012**, 51, 9994.
[4] J. B. Goodenough, *Energ. Stor. Mater.* **2015**, 1, 158.
[5] Y. Zhang, Y. Huang, J. A. Rogers, *Curr. Opin. Solid State Mater. Sci.* **2015**, 19, 190.
[6] C. Choi, S. H. Kim, H. J. Sim, J. A. Lee, A. Y. Choi, Y. T. Kim, X. Lepró, G. M. Spinks, R. H. Baughman, S. J. Kim, *Sci. Rep.* **2015**, 5, 9387.
[7] M. D. Lima, N. Li, M. Jung de Andrade, S. Fang, J. Oh, G. M. Spinks, M. E. Kozlov, C. S. Haines, D. Suh, J. Foroughi, S. J. Kim, Y. Chen, T. Ware, M. K. Shin, L. D. Machado, A. F. Fonseca, J. D. Madden, W. E. Voit, D. S. Galvao, R. H. Baughman, *Science* **2012**, 338, 928.
[8] J. Yu, W. Lu, J. P. Smith, K. S. Booksh, L. Meng, Y. Huang, Q. Li, J. H. Byun, Y. Oh, Y. Yan, *Adv. Energ. Mater.* **2016**, DOI: 10.1002/aenm.201600976.
[9] J. Song, *Curr. Opin. Solid State Mater. Sci.* **2015**, 19, 160.
[10] C. Wang, W. Zheng, Z. Yue, C. O. Too, G. G. Wallace, *Adv. Mater.* **2011**, 23, 3580.
[11] D. H. Kim, J. Song, W. M. Choi, H. S. Kim, R. H. Kim, Z. Liu, Y. Y. Huang, K. C. Hwang, Y. W. Zhang, J. A. Rogers, *Proceedings of the National Academy of Sciences of the United States of America* **2008**, 105, 18675.
[12] Y. Zhang, S. Wang, X. Li, J. A. Fan, S. Xu, Y. M. Song, K. J. Choi, W. H. Yeo, W. Lee, S. N. Nazaar, *Adv. Fun. Mater.* **2014**, 24, 2028.
[13] S. Xu, Y. Zhang, J. Cho, J. Lee, X. Huang, L. Jia, J. A. Fan, Y. Su, J. Su, H. Zhang, H. Cheng, B. Lu, C. Yu, C. Chuang, T. I. Kim, T. Song, K. Shigeta, S. Kang, C. Dagdeviren, I. Petrov, P. V. Braun, Y. Huang, U. Paik, J. A. Rogers, *Nat. Commun.* **2013**, 4, 1543.
[14] B. Yue, C. Wang, X. Ding, G. G. Wallace, *Electrochim. Acta.* **2013**, 113, 17.
[15] Z. Yang, J. Deng, X. Chen, J. Ren, H. Peng, *Angew. Chem. Int. Ed.* **2013**, 52, 13453.
[16] C. Yu, C. Masarapu, J. Rong, B. Wei, H. Jiang, *Adv. Mater.* **2009**, 21, 4793.
[17] Z. Niu, H. Dong, B. Zhu, J. Li, H. H. Hng, W. Zhou, X. Chen, S. Xie, *Adv. Mater.* **2013**, 25, 1058.
[18] T. Chen, H. Peng, M. Durstock, L. Dai, *Sci. Rep.* **2014**, 4, 3612.
[19] Z. Lu, Y. Chao, Y. Ge, J. Foroughi, Y. Zhao, C. Wang, H. Long, G. G. Wallace, *Nanoscale* **2017**, 9, 5063.
[20] S. Zhang, K. K. Koziol, I. A. Kinloch, A. H. Windle, *Small* **2008**, 4, 1217.
[21] N. Behabtu, C. C. Young, D. E. Tsentalovich, O. Kleinerman, X. Wang, A. W. Ma, E. A. Bengio, R. F. ter Waarbeek, J. J. de Jong, R. E. Hoogerwerf, *Science* **2013**, 339, 182.
[22] L. M. Ericson, H. Fan, H. Peng, V. A. Davis, W. Zhou, J. Sulpizio, Y. Wang, R. Booker, J. Vavro, C. Guthy, A. N. Parra-Vasquez, M. J. Kim, S. Ramesh, R. K. Saini, C. Kittrell, G. Lavin, H. Schmidt, W. W. Adams, W. E. Billups, M. Pasquali, W. F. Hwang, R. H. Hauge, J. E. Fischer, R. E. Smalley, *Science* **2004**, 305, 1447.
[23] M. Zhang, K. R. Atkinson, R. H. Baughman, *Science* **2004**, 306, 1358.
[24] D. Yu, L. Dai, *J Phys Chem Lett.* **2009**, 1, 467.
[25] N. Jha, P. Ramesh, E. Bekyarova, M. E. Itkis, R. C. Haddon, *Adv. Energ. Mater.* **2012**, 2, 438.
[26] T. Chen, R. Hao, H. Peng, L. Dai, *Angew. Chem. Int. Ed.* **2015**, 54, 618.
[27] Z. Zhang, J. Deng, X. Li, Z. Yang, S. He, X. Chen, G. Guan, J. Ren, H. Peng, *Adv. Mater.* **2015**, 27, 356.
[28] C. Choi, K. M. Kim, K. J. Kim, X. Lepró, G. M. Spinks, R. H. Baughman, S. J. Kim, *Nature Communications* **2016**, 7, 13811.
[29] W. Lu, S. Liu, X. Qin, L. Wang, J. Tian, Y. Luo, A. M. Asiri, A. O. Al-Youbi, X. Sun, *J. Mater. Chem.* **2012**, 22, 8775.
[30] J. Melin, G. Furdin, H. Fuzellier, R. Vasse, A. Herold, *Mater. Sci. Eng.* **1977**, 31, 61.
[31] N. Behabtu, J. R. Lomeda, M. J. Green, A. L. Higginbotham, A. Sinitskii, D. V. Kosynkin, D. Tsentalovich, A. N. G. Parra-Vasquez, J. Schmidt, E. Kesselman, *Nat. nanotec.* **2010**, 5, 406.

[32] A. Rinzler, J. Liu, H. Dai, P. Nikolaev, C. Huffman, F. Rodriguez-Macias, P. Boul, A. Lu, D. Heymann, D. Colbert, *Appl. Phys. A Mate.r Sci. Process.* **1998**, 67, 29.
[33] J. Liu, A. G. Rinzler, H. Dai, J. H. Hafner, R. K. Bradley, P. J. Boul, A. Lu, T. Iverson, K. Shelimov, C. B. Huffman, *Science* **1998**, 280, 1253.
[34] G. Eda, G. Fanchini, M. Chhowalla, *Nat. nanotec.* **2008**, 3, 270.
[35] S. D. Sarma, S. Adam, E. Hwang, E. Rossi, *Rev Mod Phys.* **2011**, 83, 407.
[36] J. Foroughi, D. Antiohos, G. G. Wallace, *RSC Advances* **2016**, 6, 46427.
[37] A. M. Bryan, L. M. Santino, Y. Lu, S. Acharya, J. M. D'Arcy, *Chemistry of Materials* **2016**, 28, 5989.
[38] J. Foroughi, G. M. Spinks, G. G. Wallace, *Handbook of Smart Textiles* **2015**, 31.
[39] X. Chen, H. Lin, J. Deng, Y. Zhang, X. Sun, P. Chen, X. Fang, Z. Zhang, G. Guan, H. Peng, *Adv. Mater.* **2014**, 26, 8126.
[40] H. Peng, *Fiber-shaped energy harvesting and storage devices*, Springer, Berlin **2015**.
[41] C. Meng, C. Liu, S. Fan, *Electrochem. Commum,* **2009**, 11, 186.
[42] C. Choi, J. H. Kim, H. J. Sim, J. Di, R. H. Baughman, S. J. Kim, *Adv. Energ. Mater.* **2017**, 7, 1602021.
[43] S. H. Ng, J. Wang, D. Wexler, K. Konstantinov, Z. P. Guo, H. K. Liu, *Angew. Chem. Int. Ed.* **2006**, 45, 6896.
[44] J. Foroughi, G. M. Spinks, S. Aziz, A. Mirabedini, A. Jeiranikhameneh, G. G. Wallace, M. E. Kozlov, R. H. Baughman, *ACS nano* **2016**, 10, 9129.
[45] X. Chen, L. Qiu, J. Ren, G. Guan, H. Lin, Z. Zhang, P. Chen, Y. Wang, H. Peng, *Adv. Mater.* **2013**, 25, 6436.
[46] P. Xu, B. Wei, Z. Cao, J. Zheng, K. Gong, F. Li, J. Yu, Q. Li, W. Lu, J.-H. Byun, *ACS nano* **2015**, 9, 6088.
[47] H. Wang, Z. Liu, J. Ding, X. Lepró, S. Fang, N. Jiang, N. Yuan, R. Wang, Q. Yin, W. Lv, *Adv. Mater.* **2016**, 28, 4998.
[48] P. Xu, T. Gu, Z. Cao, B. Wei, J. Yu, F. Li, J. H. Byun, W. Lu, Q. Li, T. W. Chou, *Adv. Energ. Mater.* **2014**, 4, 1300759.

Figures and tables

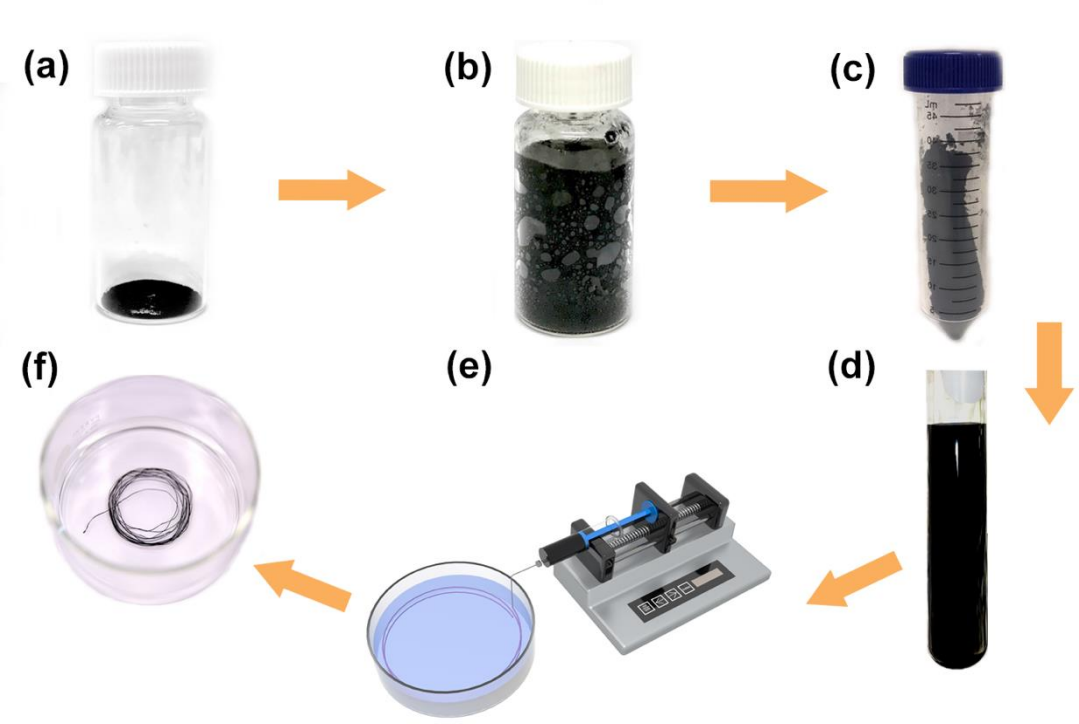

Figure 1. Schematic illustration of the fabrication of the wet-spun CNT/Graphene hybrid fiber: the multi-layer graphene platelets, (a) before treatment, (b) after treatment with CSA and H_2O_2, (c) washed and dried products by freeze drying, (d) as-prepared CNT/Graphene/CSA liquid-crystal spinning solution, (e) wet-spinning set-up, and (f) as-prepared hybrid CNT/graphene fiber by extruding spinning solution into acetone as coagulation bath.

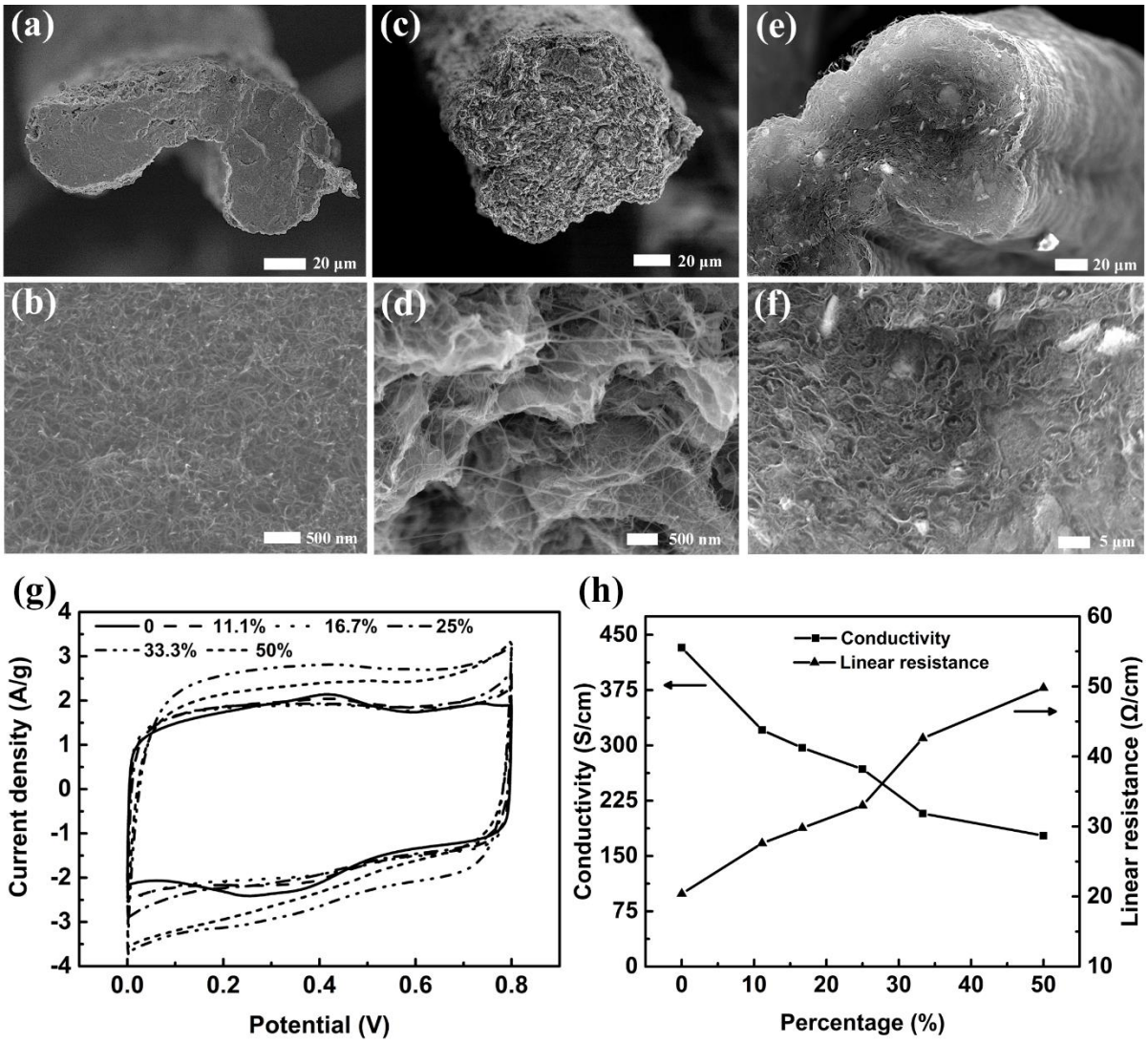

Figure 2. The SEM images of a cross-section of wet-spun pristine CNT fiber at: (a) low and (b) higher magnification. (c) Cross-section of wet-spun hybrid CNT/Graphene fiber at low and (d) higher magnification, the ratio of graphene was 33.3%. (e) Cross-section of wet-spun hybrid CNT/Graphene fiber (wet state) at low and (f) higher magnification. (g) The Cyclic voltammograms of different ratios of graphene in hybrid fiber at a scan rate of 50 mV s^{-1} in 1 M H_2SO_4, and (h) the electrical conductivity and linear resistance of developed fibers as a function of percentage of the graphene (%wt).

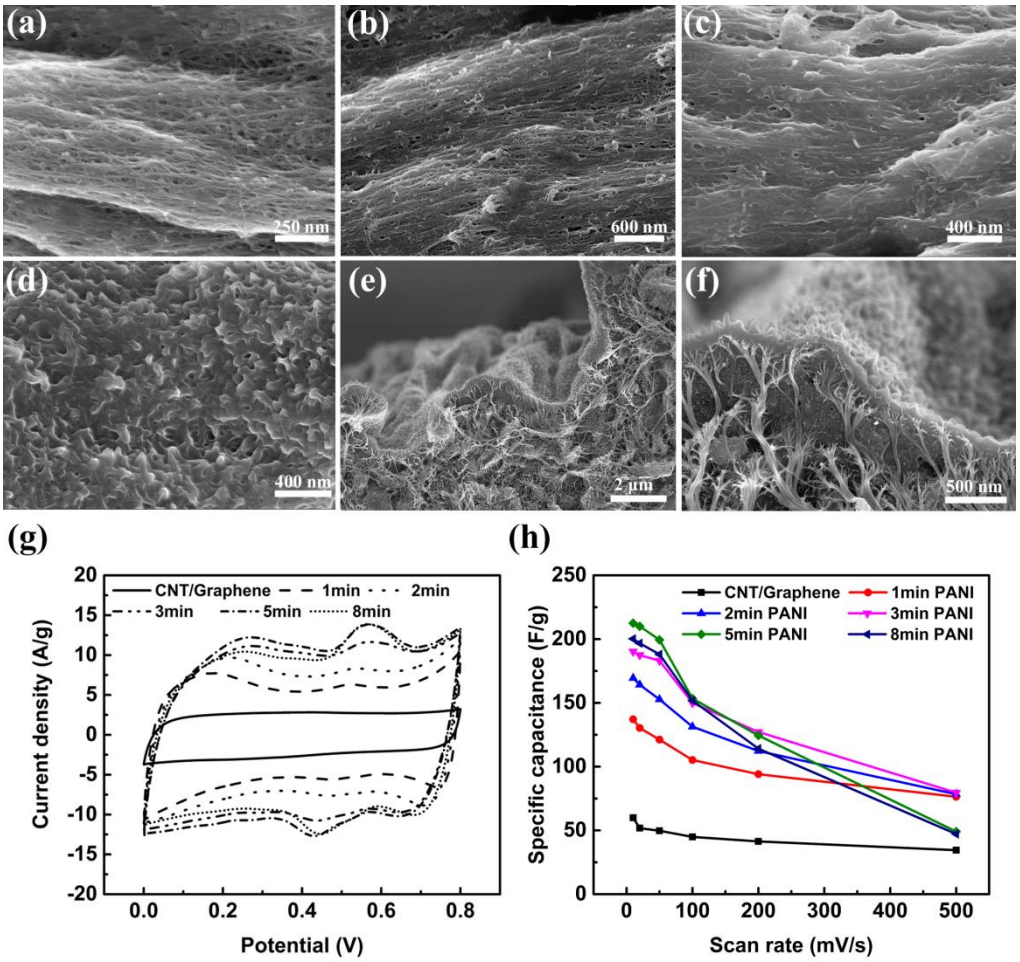

Figure 3. (a) The surface morphology of as-prepared CNT/Graphene fiber, and the PANi deposited CNT/Graphene fibers with different electrodeposition time of: (b) 1 min, (c) 5 min, and (d) 8 min. (e), (f) The SEM images of the cross-section of PANI deposited hybrid fiber with 8 min deposition time, showing a thickness of deposited layer and the arrays of PANI. (g) Cyclic voltammograms of different electrodeposition times of PANI at a scan rate of 50 mV s^{-1} from 0 to 0.8 V, (h) capacitances of supercapacitor with different electrodeposition times at a scan rate ranging from 10 mV s^{-1} to 500 mV s^{-1}.

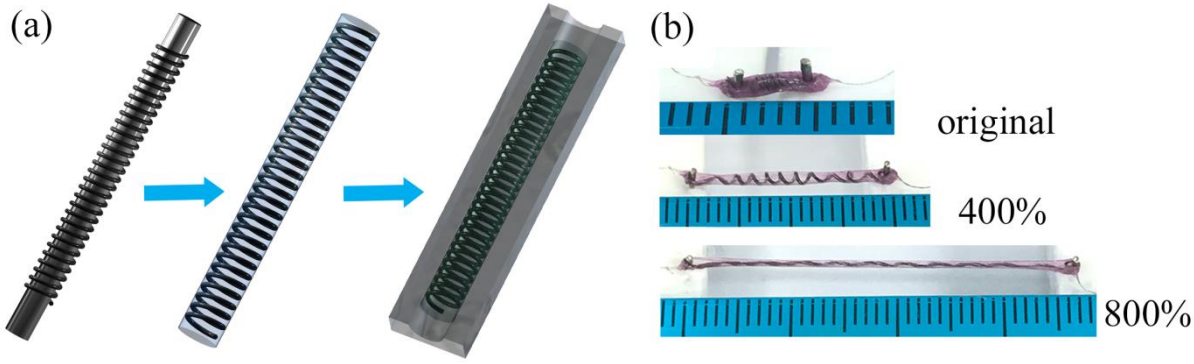

Figure 4. (a) Schematic illustration of the fabrication of a superelastic fiber-based supercapacitor, in which a yarn like supercapacitor is coiled on a rod and then cast with a thin layer of SEBS polymer to fix the spring structure, and finally the rod is removed and the device is placed in a mould to be thoroughly covered with rubber. (b) Illustration of prepared supercapacitor with different strains up to 800%.

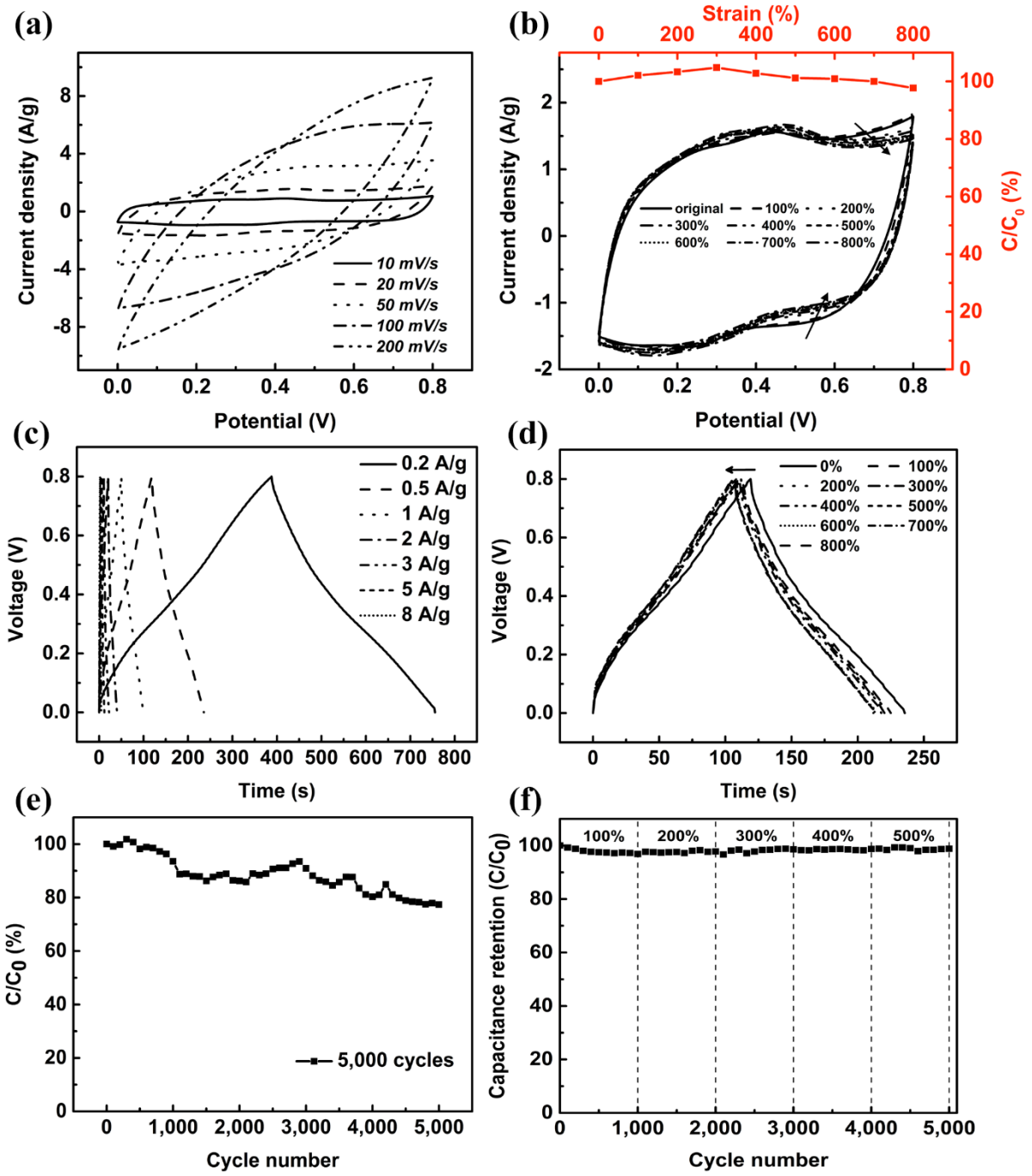

Figure 5. (a) Cyclic voltammograms of the best CNT/Graphene/PANi hybrid fiber supercapacitor. (b) Cyclic voltammograms and capacitance retention of the stretchable hybrid fiber-based supercapacitor with different tensile strains at 20 mV s^{-1}. (c) Galvanostatic charge-discharge curves of a single supercapacitor, and (d) charge-discharge curves of the

supercapacitor at different tensile strains under a current density of 0.5 A/g. (e) Capacitance retention after long cycles charge-discharge at 800% tensile strain. (f) Capacitance retention with respect to stretch cycle numbers with different tensile strain from 100% to 500%.

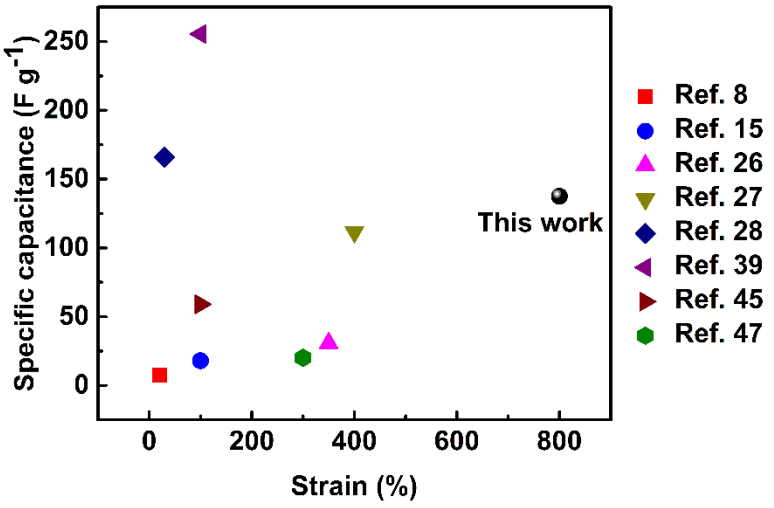

Figure 6. Comparison of the specific capacitance and the maximum reversible tensile strain for present hybrid CNT/Graphene/PANi fiber supercapacitor and previous reported stretchable supercapacitors.

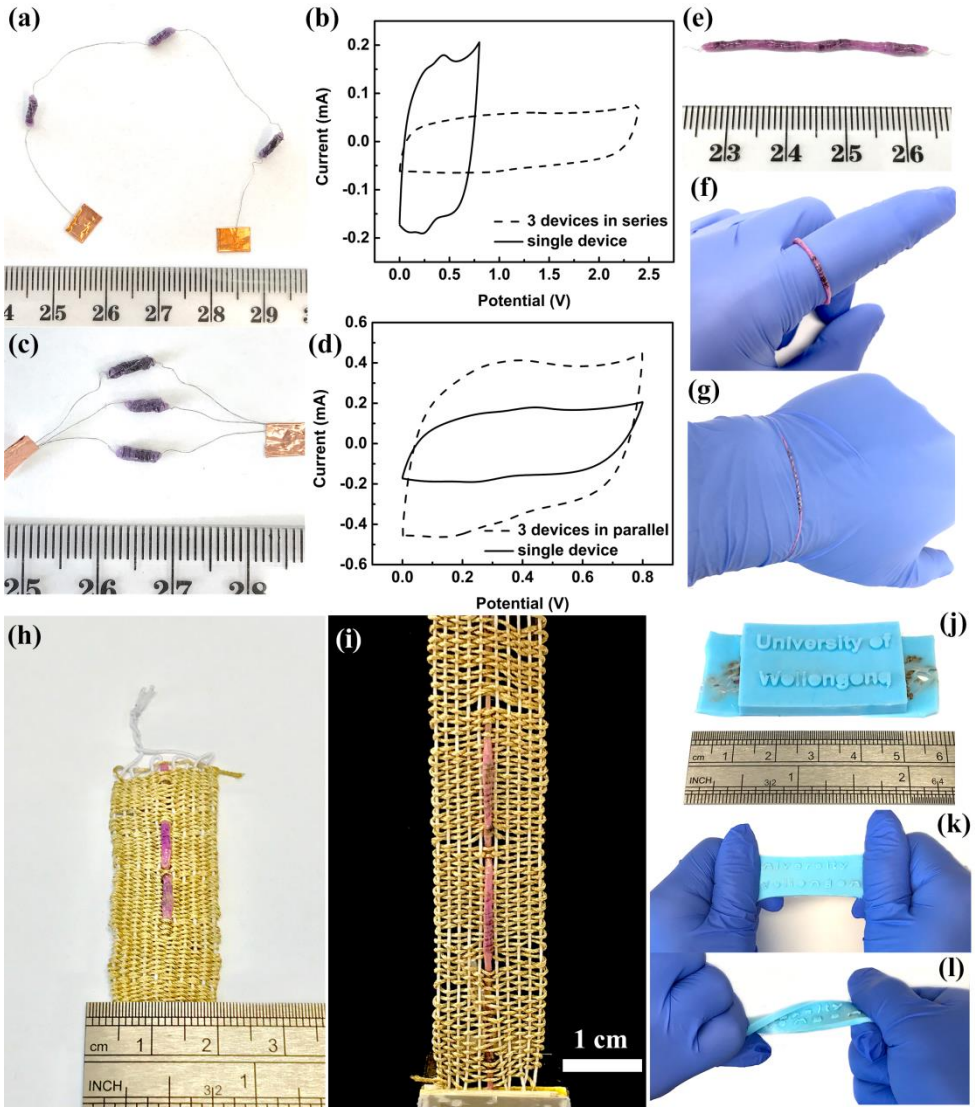

Figure 7. (a) Illustration and (b) CV curves of supercapacitors in series and (c), (d) in parallel. (e) Demonstration of a sealed stretchable supercapacitor with four devices in series with an application as (f) a ring or (g) wrist band and (h), (i) it can also be integrated in a stretchable textile. (j) The textile can be further composited with silicone, which can be (k) stretched and (l) twisted.

Table 1. Comparison of this Supercapacitor with previous stretchable supercapacitors in terms of specific capacitance and stretchability.

Materials	Fabrication methods	Electrochemical performance	Strain properties	Reference
Spring-structure CNT/Graphene/PANI fiber supercapacitor	Electrodeposit PANI onto CNT/Graphene fiber and wrap the supercapacitor as a spring structure, then coat with elastic polymer	137.5 F g^{-1} at 1 A g^{-1} (10.3 mF cm^{-1}, 273.7 mF cm^{-2}, 91.2 F cm^{-3}) 106.3 F g^{-1} after 5,000 cycles with 800% strain	Over 800%	This work
Coiled CNT/MnO_2/Polymer Fiber	Nylon core coated with CNT/ MnO_2 shell, coiled structure	5.4 mF cm^{-1}, 40.9 mF cm^{-2}, 3.8 F cm^{-3}	maximum: 150% strain	[6]
CNT/MnO_2 fiber/CNT/PPy film asymmetric supercapacitor	Core- solid-state spun CNT/MnO_2 fiber Sheath- CNT/PPy film With helical structure	60.43 mF cm^{-2} (7.72 F g^{-1}, 9.46 F cm^{-3}, 19.86 mF cm^{-1})	20% strain	[8]
CNT/rubber	Wrapping CNT on elastic fiber	18 F g^{-1}	stretching 100%	[15]
Sheath-core CNT/elastic wire /PEDOT:PSS	Core-elastic wire Sheath- CNT sheets coated with PEDOT:PSS	up to 30.7 F g^{-1}	up to 350% strain	[26]
CNT/elastic polymer /PANI	Deposited PANI on the CNT sheet coated elastic polymer fiber	111.6 F g^{-1} 79.4 F g^{-1} after 5,000 cycles with 300% strain 100.8 F g^{-1} after bending for 5,000 cycles	over 400% strain	[27]
Superelastic biscrolled yarn supercapacitor	Biscroll MnO_2 nanopaticles with CNT sheets and then over twist	17.7 mF cm^{-1}, 382.2 mF cm^{-2}, 104.7 F cm^{-3}, 166 F g^{-1}	Up to 30%	[28]
CNT/rubber fiber/PANI	Electrodeposit PANI onto CNT fiber	255.5 F g^{-1}	maximum: 100% strain	[39]
Coaxial CNT fiber	Solid state spun	59 F g^{-1}, 8.66 mF cm^{-2}	100% strain	[45]
CNT fiber/ CNT/MnO_2 fiber asymmetric supercapacitor	Solid-state spun CNT fiber coated with MnO_2	157.53 μF cm^{-1} at 50 mV s^{-1},	Up to 100% strain	[46]
Sheath-core CNT/rubber	Core-rubber Sheath- CNT sheets	20.1 F g^{-1}	300% strain	[47]
CNT/spandex wire shaped	Pre-straining-then-buckling approach	4.63−4.99 mF cm^{-2}	100% strain	[48]

Supporting Information

Superelastic hybrid CNT/Graphene fibers for wearable energy storage

Zan Lu[1, 2, 3], Javad Foroughi[*2, 4], Caiyun Wang[2], Hairu Long[1, 3], Gordon G. Wallace[*2]

1. College of Textiles, Donghua University, 2999 North Renmin Road, Shanghai, China.

2. Intelligent Polymer Research Institute, ARC Centre of Excellence for Electromaterials Science, University of Wollongong, NSW 2522, Australia.

3. Engineering Research Center of Technical Textile, Ministry of Education, Shanghai, China.

4. Illawarra Health and Medical Research Institute, University of Wollongong, NSW 2522, Australia.

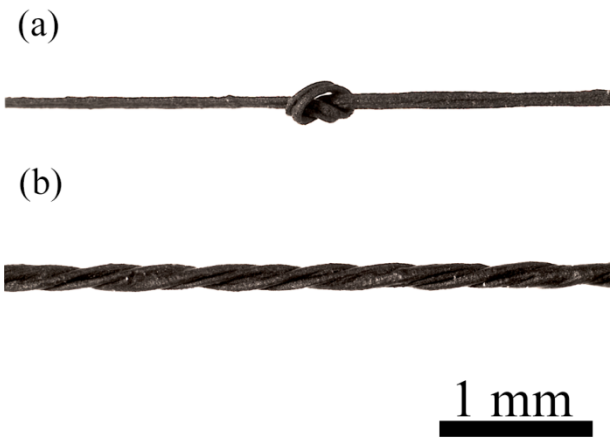

Figure S1. As-prepared the CNT/Graphene hybrid fiber can be: (a) tied as a knot or (b) twisted as a two-ply yarn without any damage to the fibers.

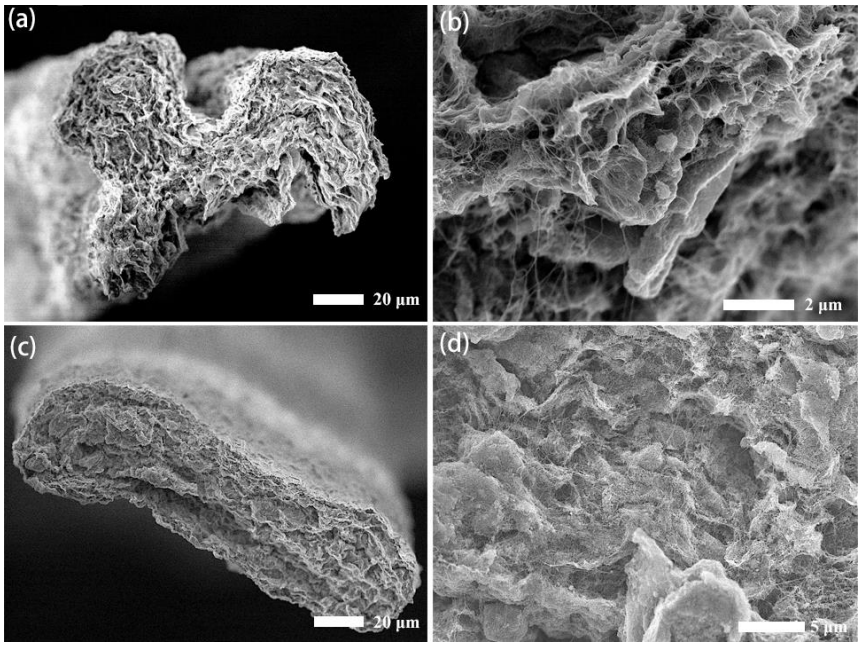

Figure S2. Cross-section morphologies of CNT/Graphene fiber with different ratios of (a), (b) 1:5, and (c), (d) 1:1, the ratio is defined as graphene to CNT.

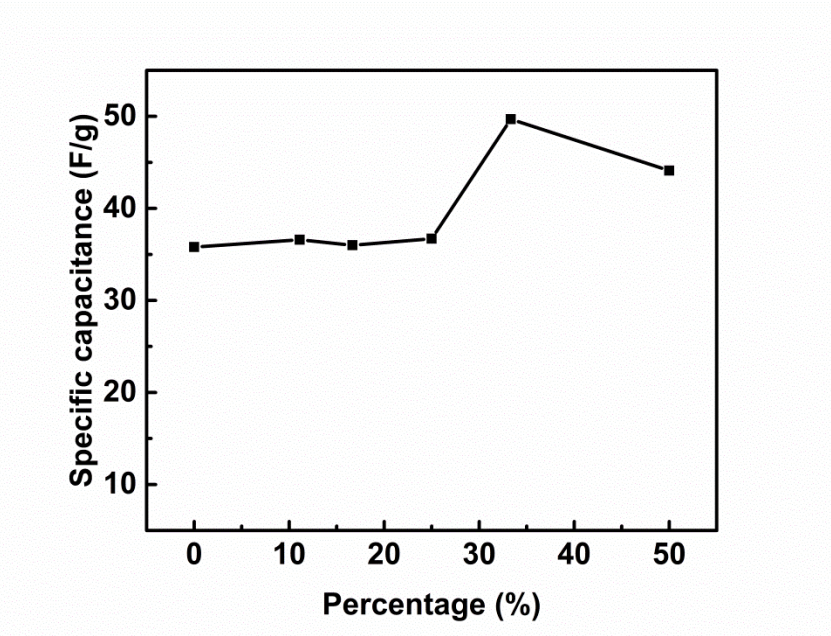

Figure S3. Specific capacitances calculated from the CV curves with different percentages of graphene in CNT/Graphene hybrid fiber.

The specific capacitance of a single electrode in the three-electrode system was calculated by using the CV curves according to the following equation:

$$C_m = \frac{Idt}{mdV}$$

where I is the average current during discharge (from V_{max} to zero volts) and dV/dt is the scan rate, m is the mass of the active materials in working electrode. The specific capacitance of a solid state supercapacitor was calculated from galvanostatic charge-discharge curves using:

$$C = \frac{2I\Delta t}{m\Delta V}$$

where Δt (s) is the discharge time, $I(A)$ is the current applied on one electrode, m (g) is the mass of one electrode in the symmetric supercapacitor, $\Delta V(V)$ is the potential window of the discharging process.

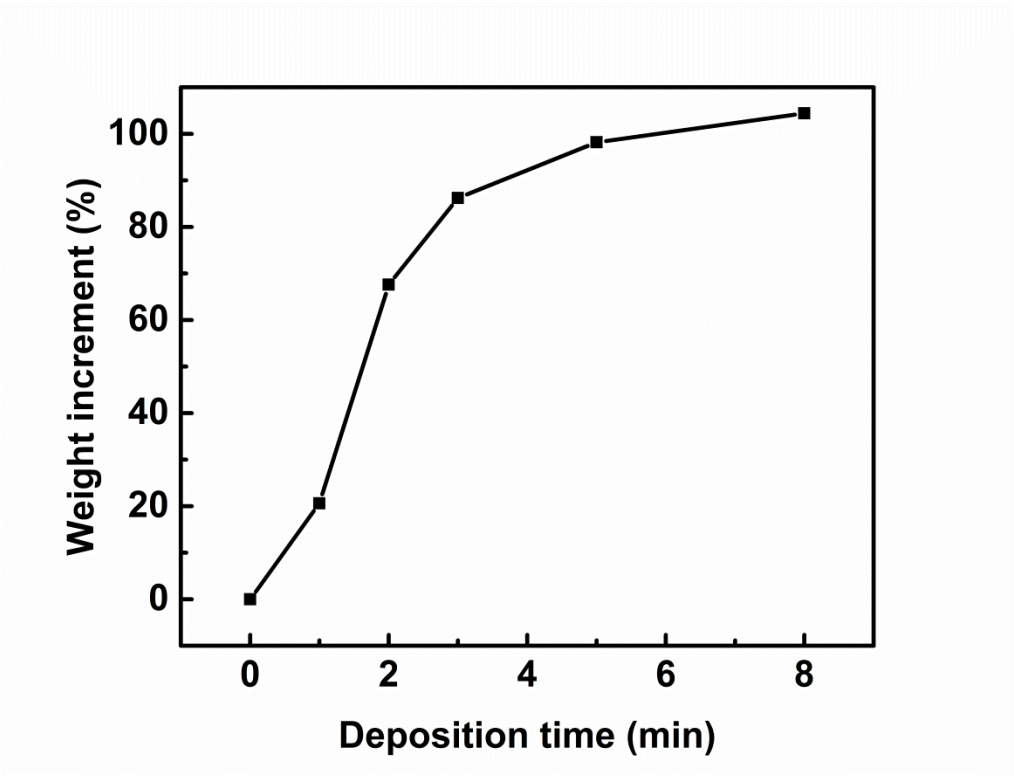

Figure S4. The weight increment of PANi deposited CNT/Graphene hybrid fiber with different electrodeposition times ranging from 0 to 8 min.

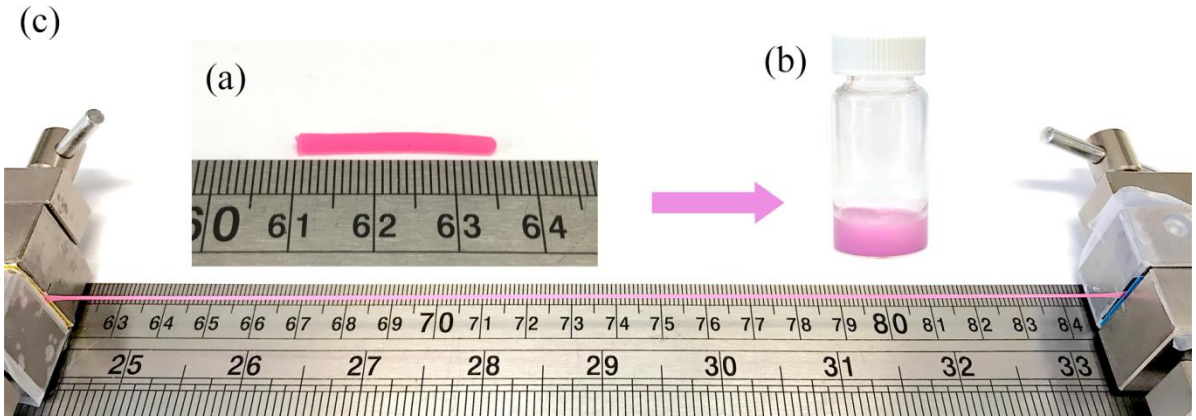

Figure S5. (a) Commercial SEBS based elastic rubber, which can be easily dissolved in (b) cyclohexane. (c) The rubber can be stretched as high as 900 %, showing an excellent stretchability.

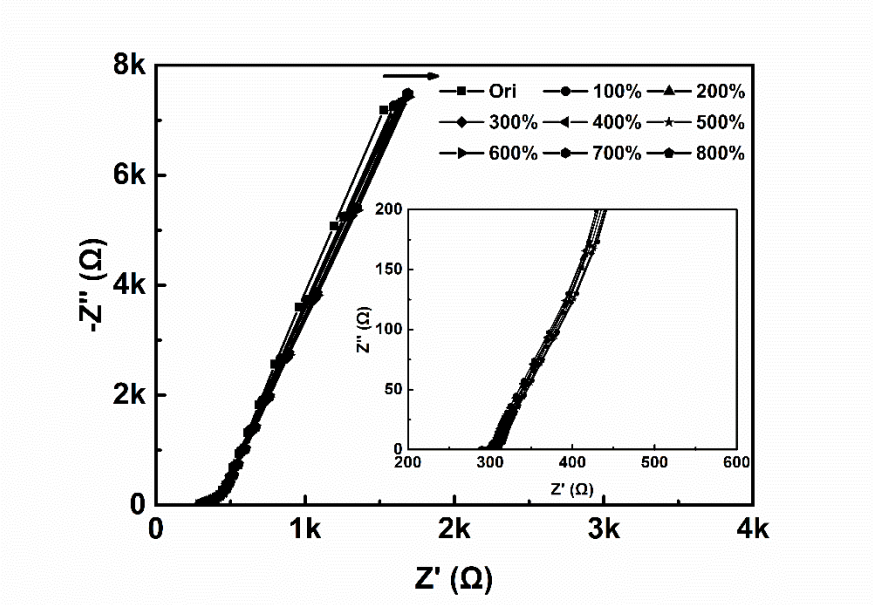

Figure S6 Nyquist plots of the stretchable supercapacitor with the length from original to 800% strain; the inset shows the expanded view of the high frequency range.

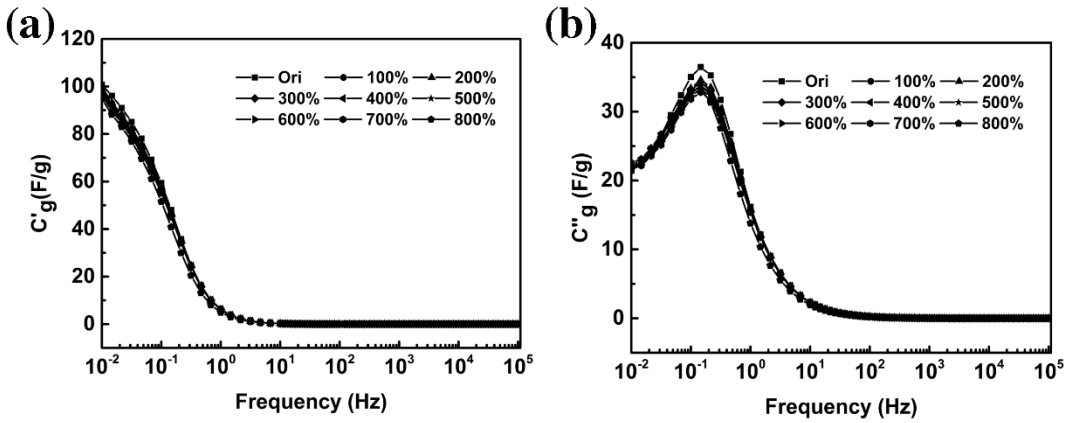

Figure S7 (a) Bode plots of the real gravimetric specific capacitance. (b) Bode plots of imaginary gravimetric specific capacitance related to the relaxation time constants. Both are calculated from EIS data for the stretchable supercapacitor with the length from original to 800% strain.

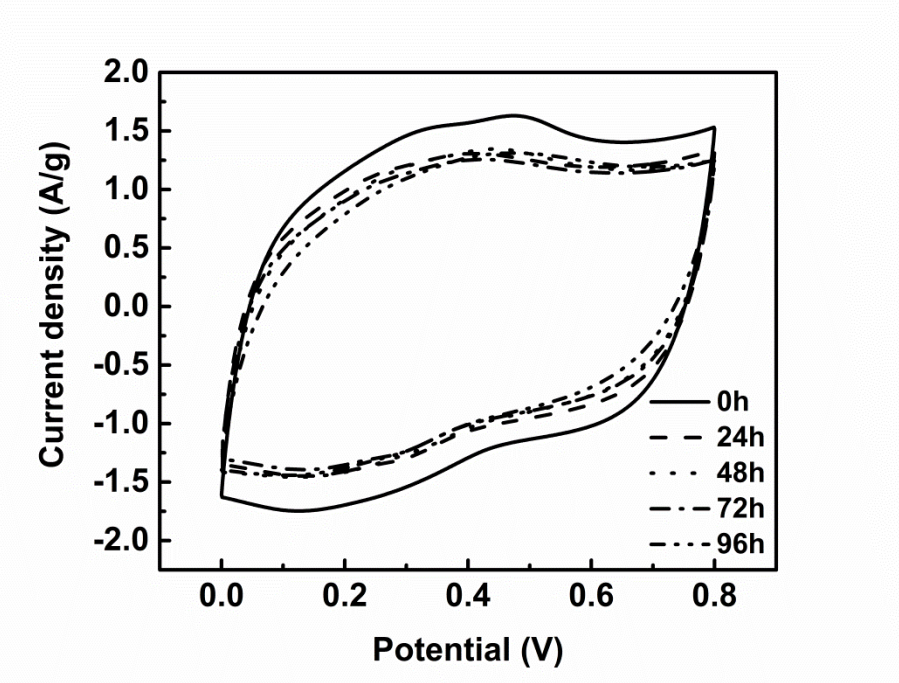

Figure S8. Cyclic voltammograms of the supercapacitor after 400% prolonged tensile strain from 24h, 48h, 72h to 96h respectively, at a scan rate of 20 mV s^{-1} in a two-electrode system.

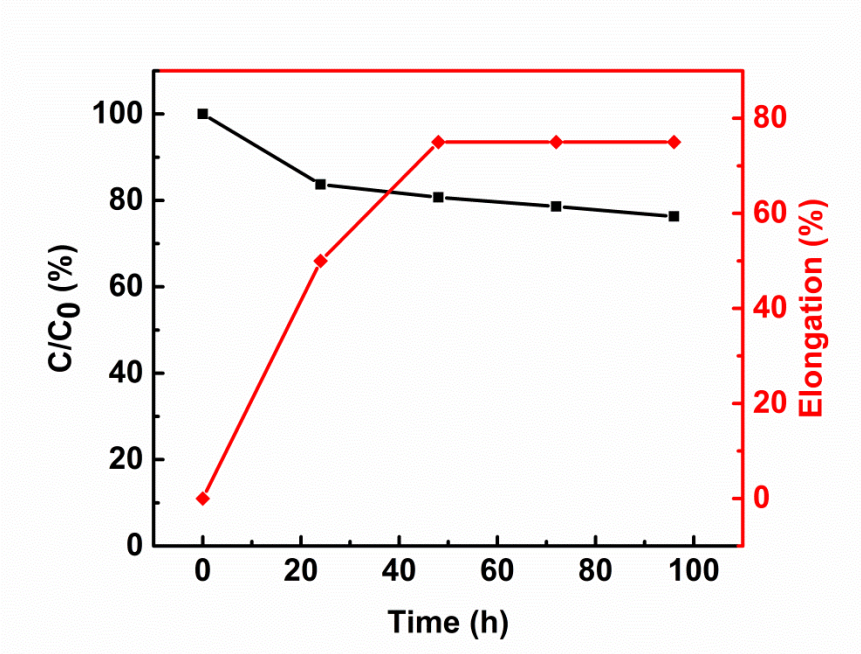

Figure S9. Capacitance retention and the elongation of supercapacitor after 400% prolonged strain from 24h, 48h, 72h to 96h.

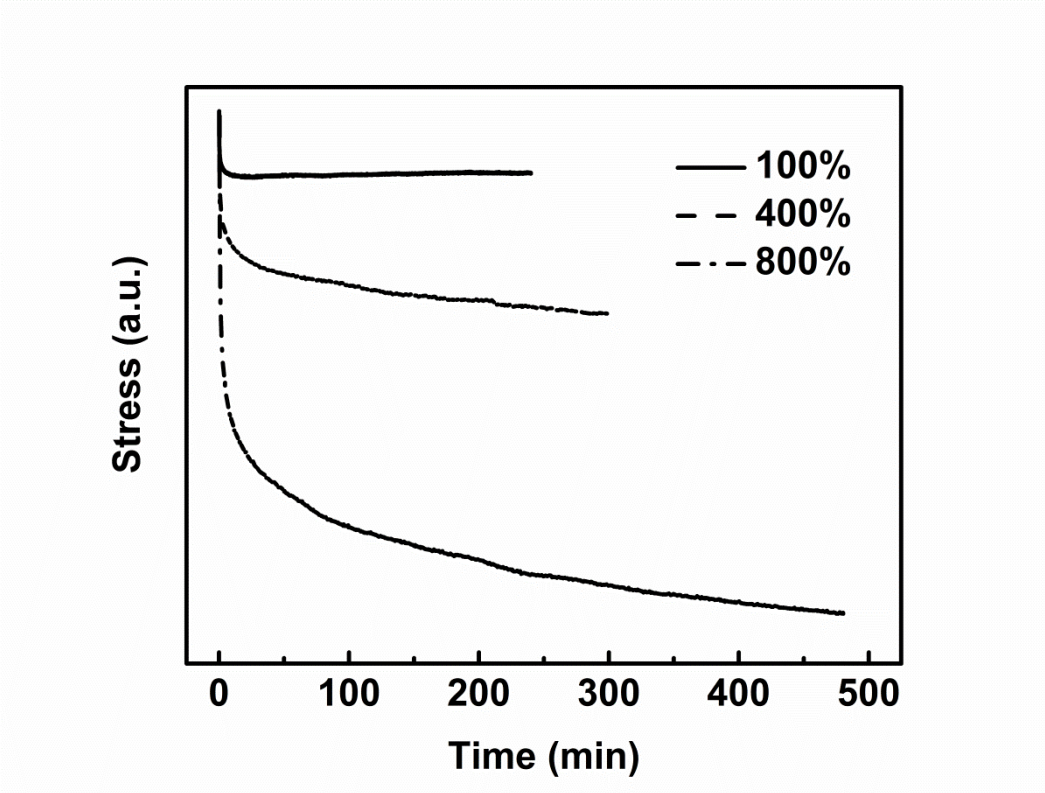

Figure S10. Mechanical property of stress relaxation which was tested under constant strain of 100%, 400% and 800%, respectively.

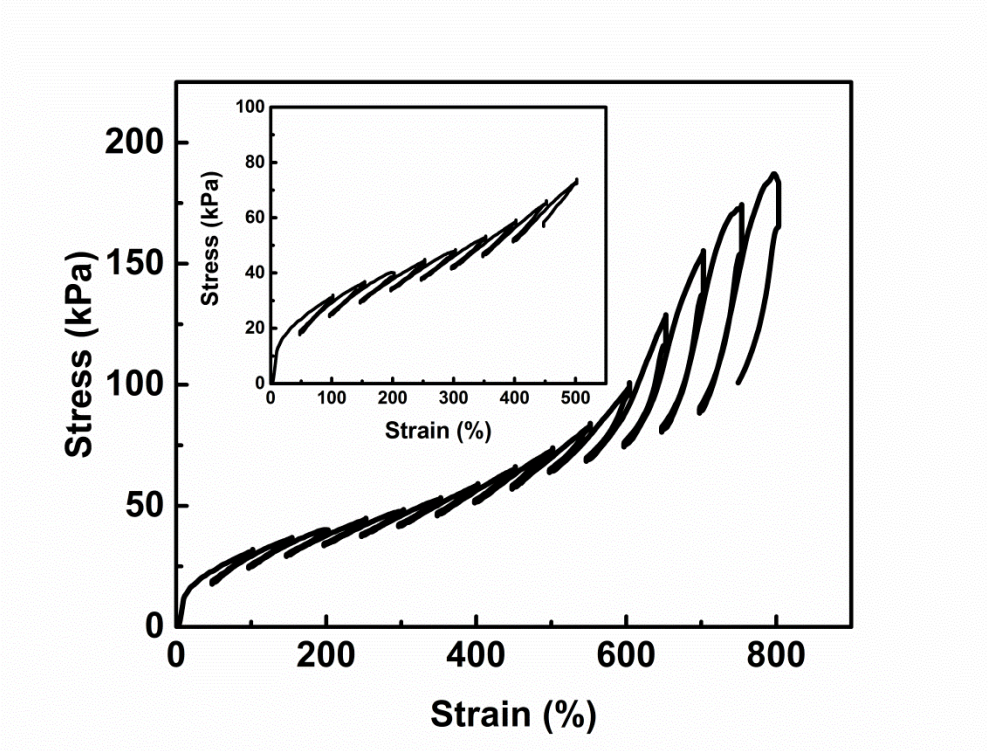

Figure S11. Stress-strain curves (stretch rate 100 mm/min with 50% strain of each load) observed on unloading and reloading a stretchable fiber-based supercapacitor over an 800% strain range after differing initial strains. (Inset: hysteretic stress-strain curves up to 500% strain.)

Stress relaxation and cyclic loading-unloading tensile test were applied by a tensile testing instrument (Shimadzu EZ-L, 10 N load cell and 10 N clamps). Stress relaxation was measured at fixed strains of 100%, 400% and 800%, while the cyclic stretch property was taken under a constant rate of 100 mm/min with 50% strain of each cycle.